VNU Journal of Science: Mathematics - Physics

Journal homepage: https://js.vnu.edu.vn/MaP

Original Article

Effect from Surfactant to Interfacial Tension of Ternary Bose-einstein Condensates

Nguyen Van Thu*, Tran Thi Cuc

Hanoi Pedagogical University 2, 32 Nguyen Van Linh, Xuan Hoa, Phu Tho, Vietnam

Received 04th November 2025
Revised 15th January 2026; Accepted 9th April 2026

Abstract: We investigate the variation of interfacial tension between two-component Bose–Einstein condensates (BEC) when an additional component is embedded and acts as a surfactant. The presence of this surfactant component reduces the interfacial tension and may give rise to a critical wetting phenomenon. In the absence of the surfactant-induced reduction of interfacial tension, however, the wetting transition proceeds as a first-order phase transition.

Keywords: Ternary Bose-Einstein condensates, Wetting phase diagram, Interfacial tensions.

1. Introduction

The wetting phenomenon in Bose–Einstein condensates (BEC) was first theoretically predicted in 2004 [1], where it was demonstrated that an immiscible two-component BEC confined by a hard-wall (optical wall) potential can exhibit interfacial adsorption, with one component preferentially wetting the boundary. Subsequent studies extended this investigation to include detailed analyses of wetting behavior at both hard-wall and soft-wall boundaries [2], leading to the construction of a wetting phase diagram in the space of intrinsic atomic parameters within the framework of the Gross–Pitaevskii (GP) theory. An analytical approach was later developed in Ref. [3], employing the double-parabola approximation (DPA) introduced in Ref. [4], which enabled a tractable analytic description of the wetting transition. More recently, the prewetting phase has been investigated in detail within the DPA framework [5], providing deeper insight into the nature of the wetting phase transition in two-component BEC.

In contrast to systems with hard- or soft-wall boundaries, the possibility of a wetting phenomenon in multi-componet BEC without any external walls was introduced in a ternary BEC in Ref. [6]. Analytical solutions were obtained for the case of strong segregation between components 1 and 2,

* Corresponding author.
E-mail address: nvthu@live.com

https//doi.org/10.25073/2588-1124/vnumap.5093

where the third component can wet the interface separating them. Consequently, the thickness of the surfactant (wetting) layer was investigated at three-phase coexistence in Ref. [7] and away from coexistence, that is, in the prewetting regime, in Ref. [8]. The key finding of these works is that the wetting phase transition can be either first order or critical. A characteristic feature of these transitions is the variation of the surfactant layer thickness as the system approaches the phase transition point.

In this paper, we investigate the influence of the surfactant layer on the interfacial tension at which a critical wetting phase transition can occur. The paper is organized as follows. In Sec. 2, we briefly review the wetting phase diagram of a ternary BEC within the framework of the GP theory using the DPA. Section 3 is devoted to analyzing the variation of interfacial tension in the presence of the surfactant layer. Finally, conclusions and outlook are presented in Sec. 4.

2. Wetting Phase Diagram of a Dilute Ternary BEC

In this Section, we summarize the results for the wave functions that were presented in detail in Ref. [6, 7] and analyze the wetting phase diagram of the dilute ternary BEC. Let us consider a dilute ternary BEC, say 1, 2 and 3, restricted in a volume *V*. Without an external field, our system is described by the grand potential in form [7].

$$\Omega = \sum_{i=1}^{3} \int_V d^3\vec{r} \left\{ \psi_i^*(\vec{r}) \left[-\frac{\hbar^2}{2m_i}\nabla^2 - \mu_i \right] \psi_i(\vec{r}) + \frac{g_{ii}}{2} \left|\psi_i(\vec{r})\right|^4 \right\} + \sum_{i<j} g_{ij} \int_V d^3\vec{r} \left|\psi_i(\vec{r})\right|^2 \left|\psi_j(\vec{r})\right|^2, \quad (1)$$

where $\hbar$ is the reduced Planck constant. For component *i* (*i* =1, 2, 3), m_i, μ_i denote the atomic mass and chemical potential, respectively. The condensate wave function $\psi_i(\vec{r})$ plays the role of the order parameter and is assumed to be real in the absence of flow. The inter- $(i \neq j)$ and intraspecies interactions ($i = j$) are characterized by coupling constants. For a dilute Bose gas mixtures, these coupling constants are linear in six scattering lengths a_{ij}

$$g_{ij} = 2\pi\hbar^2 \left(\frac{1}{m_i} + \frac{1}{m_j} \right) a_{ij}. \quad (2)$$

Minimizing the grand potential (1) with respect to the wave functions yields the Gross-Pitaevskii (GP) equation [7, 9],

$$-\frac{\hbar^2}{2m_i}\nabla^2\psi_i - \mu_i\psi_i + \sum_{i'=1}^{3} g_{ii'} \left|\psi_{i'}\right|^2 \psi_i = 0, \quad (3)$$

for component *i*.

The system under consideration is assumed to be uniform in the *x* and *y* directions while along *z* axis, components 1 and 2 occupy $z < 0$ and $z > 0$, respectively. The third component is located at the interface between 1-2. Therefore, the boundary conditions are

$$\begin{aligned} &\psi_1(-\infty) = \psi_2(\infty) = 1, \\ &\psi_1(\infty) = \psi_2(-\infty) = 0, \\ &\psi_3(-\infty) = \psi_3(\infty) = 0. \end{aligned} \quad (4)$$

For convenience, we introduce the healing length $\xi_i = \hbar / \sqrt{2m_i g_{ii} n_i}$ and the relative strength of the interspecies interaction

$$K_{ij} = \frac{g_{ij}}{\sqrt{g_{ii} g_{jj}}} = \frac{m_i + m_j}{2\sqrt{m_i m_j}} \frac{a_{ij}}{\sqrt{a_{ii} a_{jj}}}, \tag{5}$$

which can be totally controlled in experiments. Assuming that the components 1 and 2 are in equilibrium with the equality of the bulk pressure

$$P_1 = P_2, P_i = \frac{\mu_i^2}{2g_{ii}}, \mu_i = g_{ii} n_i \, (i = 1, 2), \tag{6}$$

with the condensed density $n_i = \psi_i^2$. Now the surfactant is put into the 1-2 interface with condensed density $\overline{n}_3$ corresponding to the chemical potential $\overline{\mu}_3$. Naturally, the conditions $\mu_3 \le \overline{\mu}_3, n_3 \le \overline{n}_3$ hold. We now introduce the dimensionless coordinate $\tilde{z} = z / \xi_2$ and reduced wave functions $\tilde{\psi}_1 = \psi_1 / \sqrt{n_1}, \tilde{\psi}_2 = \psi_2 / \sqrt{n_2}, \tilde{\psi}_3 = \psi_3 / \sqrt{\overline{n}_3}$. We restrict our attention to the case in which components 1 and 2 are in the strong segregation, i.e. $a_{12} \to \infty$. In this regime, the wave functions of condensates 1 and 2 are mutually exclusive and do not overlap each other. Their interface formed by them is located at $z = 0$.

In order to have analytical results, the DPA is invoked. To this end, we first extract the GP potential density from the grand potential (1)

$$V_{GP} = \sum_i \left(-\mu_i |\psi_i|^2 + \frac{g_{ii}}{2} |\psi_i|^4 \right) + \sum_{i<j} g_{ij} |\psi_i|^2 |\psi_j|^2. \tag{7}$$

Using the above dimensionless quantities, Eq. (3) allows us to define the reduced GP potential density from Eq. (7)

$$\tilde{V}_{GP} = \frac{V_{GP}}{g_{22} n_2^2 / 2} = -\tilde{\psi}_1^2 - \tilde{\psi}_2^2 - \frac{\mu_3}{\overline{\mu}_3} \tilde{\psi}_3^2 + \frac{\tilde{\psi}_1^4}{2} + \frac{\tilde{\psi}_2^4}{2} + \frac{\tilde{\psi}_3^4}{2}. \tag{8}$$

The typical configuration for our system is that there are two intersection points of the wave functions of condensates: $\tilde{\psi}_1$ and $\tilde{\psi}_3$ intersect at $\tilde{z}^-$ whereas $\tilde{\psi}_2$ and $\tilde{\psi}_3$ intersect at $\tilde{z}^+$.

In this regard, the GP equations (8) gives analytical relations for the wave functions of condensates [6, 7]. In region $\tilde{z} < \tilde{z}^-$ the reduced GP potential (8) is expanded to second order in deviations for $\tilde{\psi}_1$ from its bulk value 1 and from zero for $\tilde{\psi}_2$, which yields

$$\tilde{\psi}_1 = 1 - A_1 e^{\sqrt{2}\frac{\xi_2}{\xi_1}\tilde{z}}, \tilde{\psi}_2 = 0, \tilde{\psi}_3 = A_3 e^{\sqrt{K_{13} - \frac{\mu_3}{\overline{\mu}_3}}\tilde{z}}. \tag{9}$$

In region $\tilde{z}^- \le \tilde{z} \le \tilde{z}^+$, $\tilde{\psi}_1$ and $\tilde{\psi}_2$ deviate from zero whereas $\tilde{\psi}_3$ is expended around its maximum value $\sqrt{\mu_3 / \overline{\mu}_3}$ and thus

$$\tilde{\psi}_1 = \begin{cases} 2B_1 \sinh\left(\sqrt{\frac{\mu_3}{\bar{\mu}_3} K_{13} - 1}\, \frac{\xi_2}{\xi_1} \tilde{z}\right), \tilde{z} < 0; \\ 0, \tilde{z} > 0, \end{cases} \tag{10}$$

$$\tilde{\psi}_2 = \begin{cases} -2C_2 \sinh\left(\sqrt{\frac{\mu_3}{\bar{\mu}_3} K_{23} - 1} \tilde{z}\right), \tilde{z} > 0; \\ 0, \tilde{z} < 0, \end{cases} \tag{11}$$

$$\tilde{\psi}_3 = \sqrt{\frac{\mu_3}{\bar{\mu}_3}} + B_3 e^{\sqrt{\frac{2\mu_3}{\bar{\mu}_3}} \frac{\xi_2}{\bar{\xi}_3} \tilde{z}} + C_3 e^{-\sqrt{\frac{2\mu_3}{\bar{\mu}_3}} \frac{\xi_2}{\bar{\xi}_3} \tilde{z}}. \tag{12}$$

The wave functions in the last domain $\tilde{z} \geq 0$ can be obtained by those in the first domain by alternating the subscripts in the wave functions

$$\tilde{\psi}_1 = 0, \tilde{\psi}_2 = 1 - D_2 e^{-\sqrt{2}\tilde{z}}, \tilde{\psi}_3 = D_3 e^{-\sqrt{K_{23} - \frac{\mu_3}{\bar{\mu}_3}} \frac{\xi_2}{\bar{\xi}_3} \tilde{z}}. \tag{13}$$

The wave functions of the components in DPA are shown in Eqs. (9)-(13), in which constants are determined by conditions for the continuity of the wave functions and their first derivatives at $\tilde{z}^-$ and $\tilde{z}^+$.

$$\begin{aligned} &\tilde{\psi}_1(\tilde{z} \to \tilde{z}^- + 0) = \tilde{\psi}_1(\tilde{z} \to \tilde{z}^- - 0), \tilde{\psi}_3(\tilde{z} \to \tilde{z}^- + 0) = \tilde{\psi}_3(\tilde{z} \to \tilde{z}^- - 0), \\ &\tilde{\psi}_2(\tilde{z} \to \tilde{z}^+ + 0) = \tilde{\psi}_2(\tilde{z} \to \tilde{z}^+ - 0), \tilde{\psi}_3(\tilde{z} \to \tilde{z}^+ + 0) = \tilde{\psi}_3(\tilde{z} \to \tilde{z}^+ - 0), \\ &\tilde{\psi}_1'(\tilde{z} \to \tilde{z}^- + 0) = \tilde{\psi}_1'(\tilde{z} \to \tilde{z}^- - 0), \tilde{\psi}_3'(\tilde{z} \to \tilde{z}^- + 0) = \tilde{\psi}_3'(\tilde{z} \to \tilde{z}^- - 0), \\ &\tilde{\psi}_2'(\tilde{z} \to \tilde{z}^+ + 0) = \tilde{\psi}_2'(\tilde{z} \to \tilde{z}^+ - 0), \tilde{\psi}_3'(\tilde{z} \to \tilde{z}^+ + 0) = \tilde{\psi}_3'(\tilde{z} \to \tilde{z}^+ - 0). \end{aligned} \tag{14}$$

Substituting Eqs. (9)-(13) into Eq. (14) one obtains 7 equations for 7 integral constants. Formulae for these constants are very long and, the most important thing is that, they do not provide any physical insights.

From the above results one finds [6-8]:

- The nucleation equation

$$\bar{\beta}_{13} + \bar{\beta}_{23} = \frac{\sqrt{2}(\xi_1 + \xi_2)}{\bar{\xi}_3} \left(\frac{\mu_3}{\bar{\mu}_3}\right)^{3/2}. \tag{15}$$

- The first-order phase transition equation

$$\xi_1 + \xi_2 = \frac{\beta_{13}(\xi_1 + \xi_3)}{\sqrt{2} + \beta_{13}} + \frac{\beta_{23}(\xi_2 + \xi_3)}{\sqrt{2} + \beta_{23}}. \tag{16}$$

- The critical phase transition equation

$$\frac{\xi_1}{\beta_{13}} + \frac{\xi_2}{\beta_{23}} = \sqrt{2}\xi_3. \tag{17}$$

In Eqs. (15) and (16) we have defined $\beta_{ij} = \sqrt{K_{ij} - 1}, \bar{\beta}_{ij} = \sqrt{K_{ij} - \frac{\mu_3}{\bar{\mu}_3}}$.

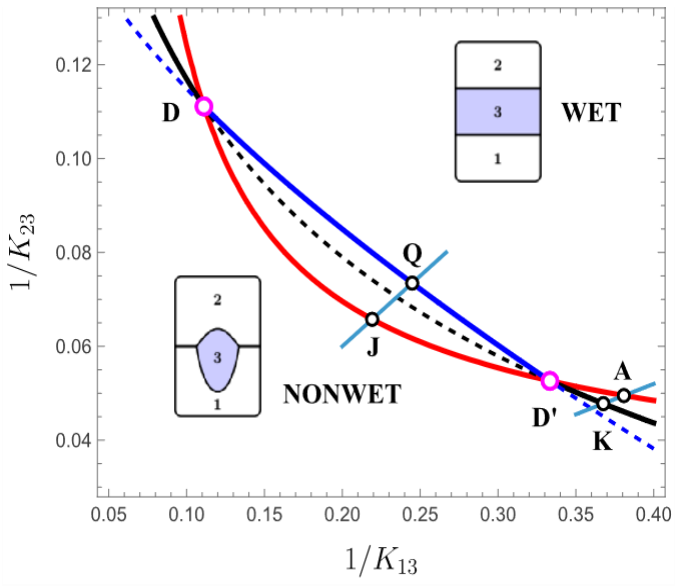

Figure 1. The wetting phase diagram in $(1/K_{13}, 1/K_{23})-$ plane at three-phase coexistence and $\xi_2/\xi_1 = 3, \xi_3/\xi_1 = 1.$

The wetting phase diagram in the $(1/K_{13}, 1/K_{23})-$plane is shown at three-phase coexistence for $\xi_2/\xi_1 = 3, \quad \xi_3/\xi_1 = 1.$ The red line represents the nucleation line corresponding to Eq. (15) at three-phase coexistence, while the black line denotes the first-order phase transition given by Eq. (16). The critical wetting transition is indicated by the blue line. The two cartoon insets illustrate the condensate configurations in the nonwet regime (below the red line), the partially wet regime (between the red and blue lines), and the completely wet regime (above the blue line). These three characteristic lines intersect at two points, D and D′, which divide the diagram into three distinct regions: the inner region located between D and D′, and the two outer regions lying above D and below D′. The points D and D' are called the degenerate points.

3. Effect of Surfactant Layer on the Interfacial Tension

It is pointed out that the wetting phase transition in the dilute ternary BEC is either first-order or critical transition [6]. In this Section we will analyze variation of the interfacial tension 1-2 while the surfactant is placed at the 1-2 interface. To this end, we first mention to the interfacial tensions in the ternary BEC. At first stage, two condensates 1 and 2 are in strong segregation and their interface locates at $\tilde{z} = 0.$ Within the DPA, the interfacial tension is [4]

$$\tilde{\gamma}_{12} = \frac{\gamma_{12}}{4P\xi_2} = \frac{1}{\sqrt{2}}\left(1 + \frac{\xi_1}{\xi_2}\right). \tag{18}$$

Right after component 3 is introduced into the 1-2 interface, its interfacial tension is reduced to $\gamma_{12(3)}$, which is defined as

$$\tilde{\gamma}_{12(3)} = \frac{\gamma_{12(3)}}{4P\xi_2} = \int\left[\left(\frac{\xi_1}{\xi_2}\frac{d\tilde{\psi}_1}{d\tilde{z}}\right)^2 + \left(\frac{d\tilde{\psi}_2}{d\tilde{z}}\right)^2 + \left(\frac{\bar{\xi}_3}{\xi_2}\frac{d\tilde{\psi}_3}{d\tilde{z}}\right)^2\right]. \tag{19}$$

Plugging Eqs. (9)-(13) into Eq. (19) yields

$$\begin{aligned}\tilde{\gamma}_{12(3)} = {} & \frac{A_1^2}{\sqrt{2}}\frac{\xi_1}{\xi_2}e^{2\sqrt{2}\frac{\xi_2}{\xi_1}\tilde{z}^-} + \frac{\bar{\xi}_3}{\xi_2}\frac{A_3^2}{2}\bar{\beta}_{13}e^{2\bar{\beta}_{13}\frac{\xi_2}{\bar{\xi}_3}\tilde{z}^-} + \frac{D_2^2}{\sqrt{2}}e^{-2\sqrt{2}\tilde{z}^+} + \frac{\bar{\xi}_3}{\xi_2}\frac{D_3^2}{2}\bar{\beta}_{23}e^{-2\bar{\beta}_{23}\frac{\xi_2}{\bar{\xi}_3}\tilde{z}^+} \\ & - B_1^2\sqrt{\frac{\mu_3}{\bar{\mu}_3}K_{13}-1}\frac{\xi_1}{\xi_2}\sinh\left(2\sqrt{\frac{\mu_3}{\bar{\mu}_3}K_{13}-1}\frac{\xi_2}{\xi_1}\tilde{z}^-\right) - \sqrt{\frac{\mu_3}{2\bar{\mu}_3}}B_3^2\frac{\bar{\xi}_3}{\xi_2}e^{2\sqrt{\frac{2\mu_3}{\bar{\mu}_3}}\frac{\xi_2}{\bar{\xi}_3}\tilde{z}^-} \\ & + \sqrt{\frac{\mu_3}{2\bar{\mu}_3}}C_3^2\frac{\bar{\xi}_3}{\xi_2}e^{-2\sqrt{\frac{2\mu_3}{\bar{\mu}_3}}\frac{\xi_2}{\bar{\xi}_3}\tilde{z}^-} + C_2^2\sqrt{\frac{\mu_3}{\bar{\mu}_3}K_{23}-1}\sinh\left(2\sqrt{\frac{\mu_3}{\bar{\mu}_3}K_{23}-1}\frac{\xi_2}{\xi_1}\tilde{z}^+\right) \\ & + \sqrt{\frac{\mu_3}{2\bar{\mu}_3}}B_3^2\frac{\bar{\xi}_3}{\xi_2}e^{2\sqrt{\frac{2\mu_3}{\bar{\mu}_3}}\frac{\xi_2}{\bar{\xi}_3}\tilde{z}^+} - \sqrt{\frac{\mu_3}{2\bar{\mu}_3}}C_3^2\frac{\bar{\xi}_3}{\xi_2}e^{-2\sqrt{\frac{2\mu_3}{\bar{\mu}_3}}\frac{\xi_2}{\bar{\xi}_3}\tilde{z}^+} - \frac{4\mu_3}{\bar{\mu}_3}B_3C_3(\tilde{z}^+ - \tilde{z}^-) \\ & - 2B_1^2\left(\frac{\mu_3}{\bar{\mu}_3}K_{13}-1\right)\tilde{z}^- + 2C_2^2\left(\frac{\mu_3}{\bar{\mu}_3}K_{23}-1\right)\tilde{z}^+.\end{aligned} \tag{20}$$

At the same time, two other interfaces are appeared when a drop of the surfactant locating at the 1-2 interface, which are 1-3 and 2-3 interfaces. In the equilibrium, these interfacial tensions are defined

$$\tilde{\gamma}_{i3} = \frac{\gamma_{i3}}{4P\xi_2} = \int d\tilde{z}\left[\left(\frac{\xi_i}{\xi_2}\frac{d\tilde{\psi}_i}{d\tilde{z}}\right)^2 + \left(\frac{\bar{\xi}_3}{\xi_2}\frac{d\tilde{\psi}_3}{d\tilde{z}}\right)^2\right], i = 1,2. \tag{21}$$

Within DPA, the interfacial tensions in Eq. (21) can be evaluated [6]

$$\tilde{\gamma}_{i3} = \frac{1}{\sqrt{2}}\frac{\beta_{i3}}{\sqrt{2}+\beta_{i3}}\frac{\xi_i+\xi_3}{\xi_2}. \tag{22}$$

We now use Eqs. (18), (20)-(22) to consider evolution of the interfacial tension $\tilde{\gamma}_{12(3)}$ in relationship with $\tilde{\gamma}_{12}, \tilde{\gamma}_{13}$ and $\tilde{\gamma}_{23}$ associating the wetting phase diagram in Fig. 1. Note that components 1 and 2 are in strong segregation therefore $\tilde{\gamma}_{12}$ in Eq. (18) is a constant. The occurrence of the wetting phase transition is determined by the magnitude of $\tilde{\gamma}_{12(3)}$ and its relative value with respect to $\tilde{\gamma}_{13}+\tilde{\gamma}_{23}$ and $\tilde{\gamma}_{12}$. It is well known that, if it occurs, the wetting phase transition can be either of first-order or critical, depending on the variation of $\tilde{\gamma}_{12(3)}$. Firstly, we investigate in a set of parameters corresponding to the inner region of Fig. 1, in which K_{13}/K_{23} is kept as a constant.

Fig. 2 shows the evolution of the interfacial tensions as functions of the control parameters at fixed $\xi_2/\xi_1 = 3, \xi_3/\xi_1 = 1$ and $K_{13} = 0.3K_{23}$. This corresponds to moving along the segment JQ in Fig. 1. In this process, the interfacial tension $\tilde{\gamma}_{12}$ remains constant, as indicated by the horizontal dashed line. The

black dashed slanted line represents $\tilde{\gamma}_{13}+\tilde{\gamma}_{23}$, while the blue solid line corresponds to $\tilde{\gamma}_{12(3)}$. As the parameter $1/K_{13}$ increases, nucleation of component 3 occurs at point J (lying on the nucleation line), where the interfacial tension $\tilde{\gamma}_{12}$ becomes $\tilde{\gamma}_{12(3)}$. The tension then decreases along the blue curve and reaches $\tilde{\gamma}_{13}+\tilde{\gamma}_{23}$ at point Q (lying on the critical wetting line). From the perspective of interfacial tension, this evolution corresponds to the path PWQ in Fig. 2. The nucleation of component 3 takes place at point N, while the wetting phenomenon emerges at point W, marking the critical wetting phase transition.

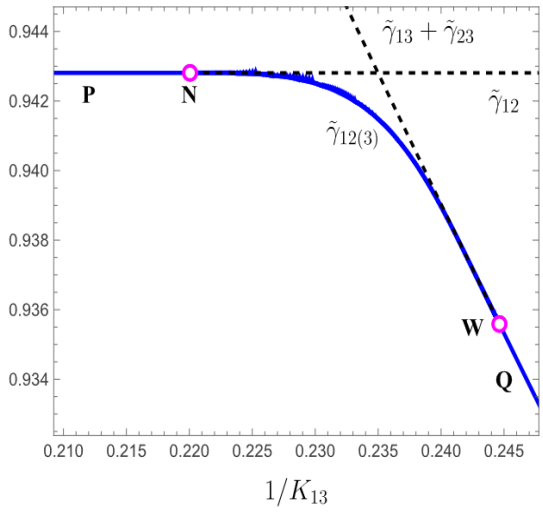

Figure 2. The evolution of the interfacial tensions as a function of $1/K_{13}$ at $\xi_2/\xi_1=3, \xi_3/\xi_1=1$ and $K_{13}=0.3K_{23}$.

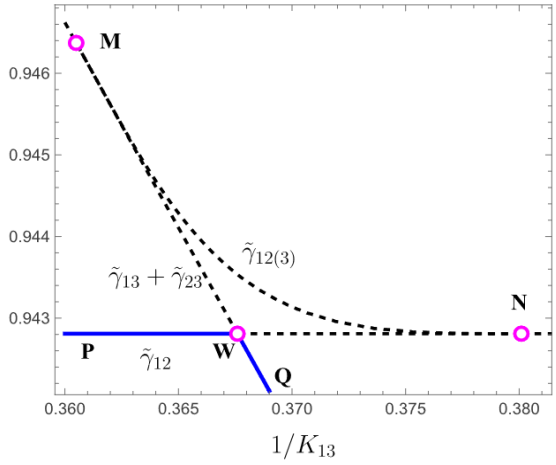

Figure 3. The evolution of the interfacial tensions as a function of $1/K_{13}$ at $\xi_2/\xi_1=3, \xi_3/\xi_1=1$ and $K_{13}=0.13K_{23}$.

We now examine the second case, in which the parameters vary along segment KA in Fig. 1, belong to the outer of the wetting region of the phase diagram. The corresponding evolution of the interfacial tensions is presented in Fig. 3. In this figure, the curves PN and MQ represent the behaviors of $\tilde{\gamma}_{12}$ and $\tilde{\gamma}_{13}+\tilde{\gamma}_{23}$, respectively, while $\tilde{\gamma}_{12(3)}$ is depicted by the curve MN. The corresponding parameters are $\xi_2/\xi_1=3, \xi_3/\xi_1=1$ and $K_{13}=0.13K_{23}$. At point A (situated on the nucleation line in Fig. 1), nucleation occurs, corresponding to point N in Fig. 3. The introduction of the surfactant results in an increase in $\tilde{\gamma}_{12(3)}$ and a decrease in $\tilde{\gamma}_{13}+\tilde{\gamma}_{23}$. This indicates that the presence of the surfactant raises the interfacial tension energy $\tilde{\gamma}_{12(3)}$ relative to $\tilde{\gamma}_{12}$, thereby violating the principle of minimum energy. Consequently, the formation of a stable surfactant layer is not energetically favorable. At point M in Fig. 3, $\tilde{\gamma}_{12(3)}=\tilde{\gamma}_{13}+\tilde{\gamma}_{23}$, during this process, the system evolves in accordance with the principle of minimum energy, following the discontinuous path represented by the broken line NWQ. At point K in Fig. 1, or equivelently point W in Fig. 3, the wetting phenomenon takes place. This discontinuity in the interfacial tension signifies that the wetting phase transition is of first order.

To close this Section, we consider behavior of the interfacial tensions off of the three-phase coexistence, i.e., the chemical potential $\mu_3 / \bar{\mu}_3 \to 1$ while other parameters are fixed at $\xi_2 / \xi_1 = 3$, $\xi_3 / \xi_1 = 1, K_{13} = 2$ and $K_{13} = 0.3K_{23}$. The evolution of these interfacial tensions are depicted in Fig. 4. The nucleation is formed at $\mu_3 / \bar{\mu}_3 = 0.857$, which corresponds to point N in Fig. 4. Upon the continuous addition of surfactant to the 1–2 interface, the corresponding interfacial tension $\tilde{\gamma}_{12(3)}$ decreases, as depicted by the blue line NW in Fig. 4. As the system approaches the three-phase coexistence, namely, when the ratio of the chemical potentials approaches unity, the interfacial tension $\tilde{\gamma}_{12(3)}$ tends toward the value $\tilde{\gamma}_{13} + \tilde{\gamma}_{23}$. This behavior serves as a clear indication of the critical wetting phase transition. This result coincides with that in Fig. 2.

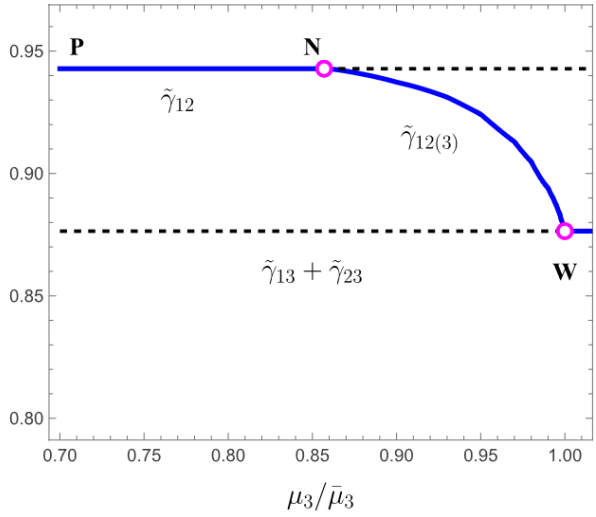

Figure 4. Behavior of the interfacial tensions as functions of the chemical potential ratio in case of the critical wetting phase transition at $\xi_2 / \xi_1 = 3, \xi_3 / \xi_1 = 1, K_{13} = 2$ and $K_{13} = 0.3K_{23}$.

4. Conclusion and Outlook

We have investigated the wetting phase transition in a dilute ternary BEC using the GP theory within the framework of DPA. The system considered involves strong segregation between components 1 and 2, whose mutual interface effectively substitutes for a hard or soft confining boundary.

The constructed wetting phase diagram, parameterized by the interspecies interaction strengths, exhibits two distinct regimes separated by degenerate boundary points. In the outer regions, the system undergoes a first-order wetting transition, whereas in the inner regions a continuous (critical) transition emerges. In the critical regime, the interfacial tension $\tilde{\gamma}_{12}$ decreases smoothly beyond the nucleation threshold and asymptotically approaches the equality condition $\tilde{\gamma}_{12(3)} = \tilde{\gamma}_{13} + \tilde{\gamma}_{23}$. This marks the formation of a thin, energetically favorable surfactant film at the interface between components 1 and 2. In contrast, in the outer regime, $\tilde{\gamma}_{12}$ remains constant, and the transition occurs abruptly once $\tilde{\gamma}_{13} + \tilde{\gamma}_{23} = \tilde{\gamma}_{12}$, which is characteristic of a first-order phase transition.

Our results demonstrate that variations in interfacial tension govern the order and mechanism of wetting transitions in multi-component condensates. The emergence of a surfactant film serves as a distinct signature of critical wetting, highlighting the intricate coupling between microscopic interspecies interactions and macroscopic interfacial behavior. Future extensions incorporating beyond-mean-field corrections or finite-temperature effects would further elucidate the interplay between quantum fluctuations and wetting phenomena in BEC mixtures.

Acknowledgments

The authors wish to thank J. O. Indekeu and J. Berx for their useful disscusions. This research is funded by Vietnam National Foundation for Science and Technology Development (NAFOSTED) under grant number 103.01-2023.12.

References

[1] J. O. Indekeu. Van Schaeybroeck, Extraordinary Wetting Phase Diagram for Mixtures of Bose-Einstein Condensates, Physical Review Letters, Vol. 93, No. 21, 2004, https://doi.org/10.1103/physrevlett.93.210402.

[2] B. V. Schaeybroeck, J. O. Indekeu, Critical Wetting, First-order Wetting, and Prewetting Phase Transitions in Binary Mixtures of Bose-Einstein Condensates, Physical Review A, Vol. 91, No. 1, 2015, https://doi.org/10.1103/physreva.91.013626.

[3] N. V. Thu, Static Properties of Bose–Einstein Condensate Mixtures in Semi-infinite Space, Physics Letters A, Vol. 380, No. 37, 2016, pp. 2920-2924, https://doi.org/10.1016/j.physleta.2016.07.017.

[4] J. O. Indekeu, C. Y. Lin, N. V. Thu, B. V. Schaeybroeck, T. H. Phat, Static Interfacial Properties of Bose-Einstein-condensate Mixtures, Physical Review A, Vol. 91, No. 3, https://doi.org/10.1103/physreva.91.033615.

[5] P. D. Thanh, N. V. Thu, Static Properties of Prewetting Phase in Binary Mixtures of Bose-Einstein Condensates, International Journal of Theoretical Physics, Vol. 63, No. 12, 2024, https://doi.org/10.1007/s10773-024-05863-w.

[6] J. O. Indekeu, N. V. Thu, J. Berx, Three-component Bose-einstein Condensates and Wetting Without Walls, Physical Review A, Vol. 111, No. 4, 2025, https://doi.org/10.1103/physreva.111.043320.

[7] N. V. Thu, D. T. Hai, Critical Wetting Phase Transition in a Dilute Ternary Bose-Einstein Condensates, VNU Journal of Science: Mathematics - Physics, 2025, https://doi.org/10.25073/2588-1124/vnumap.5037.

[8] K. Jimbo, H. Saito, Surfactant Behavior in Three-component Bose-einstein Condensates, Physical Review A, Vol. 103, No. 6, 2021, https://doi.org/10.1103/physreva.103.063323.